
IJER-INTERNATIONAL JOURNAL OF ENERGY RESEARCH

MANUSCRIPT EVALUATION

(Confidential)

Title of Paper: Modelling Micro-Turbines Using Hammerstein Models

Author(s): Francisco Jurado

Manuscript No# 030804

A) SUBJECT MATTER (Please tick where appropriate)

- | | | |
|--|---------|--------|
| 1. Is the paper a new and original contribution to the field?
(In case of a review article, is it publishable?) | YES (x) | NO () |
| 2. Is the paper relevant to the scope of IJER? | YES (x) | NO () |
| 3. Is the content of the paper properly organized? | YES (x) | NO () |
| 4. Is the length of the paper appropriate for publication? | YES (x) | NO () |
| 5. Is the paper free of the doubtful or controversial arguments? | YES (x) | NO () |
| 6. Is the paper free of the typographical and grammatical errors? | YES () | NO (x) |
| 7. Is the presentation clear to readers familiar with the field? | YES (x) | NO () |
| 8. Does the title of the paper reflect sufficiently and clearly the topic? | YES (x) | NO () |
| 9. Does the abstract contain a sufficient summary of the work done? | YES (x) | NO () |
| 10. Does the introduction present the importance of the topic,
a recent literature review, and a clear objective? | YES (x) | NO () |
| 11. Is the analysis (and/or model) clearly presented? | YES (x) | NO () |
| 12. Is the experimental part clearly presented (with an error analysis)? | YES () | NO () |
| 13. Is the discussion of the results sufficiently done? | YES (x) | NO () |
| 14. Are the conclusions sound and justifiable? | YES (x) | NO () |
| 15. Is the notation consistent with the common literature? | YES (x) | NO () |
| 16. Are the figures and tables all necessary and acceptable? | YES (x) | NO () |
| 17. Are the references adequate and appropriate? | YES (x) | NO () |

☛ Please provide further comments on the above items if necessary.

B) EVALUATION (Please tick where appropriate)

- Acceptable as it is: ()
- Acceptable with minor revisions (x)
- Acceptable with major revisions ()
- Not acceptable ()

C) REMARKS

Please see the attached sheets.

☛ Please list your additional comments on a supplementary sheet if needed.

Reviewer's name: Dr. Mehmet Sunar

Reviewer's signature:



Date: 18/11/04

Comments on the Paper
“Modelling Micro-Turbines Using Hammerstein Models” by Francisco Jurado

The paper proposes to use frequency-domain identification methods in Hammerstein modeling of Micro-Turbines and hence is recommended for publication in IJER. I have scanned the pages from the paper with my comments on them for the possible improvement to the readership. Some other comments are listed below:

- 1) It is not exactly clear to me how the block diagrams of the gas turbine and the control system are related, i.e. the relations of Figures 1 and 2 are not obvious. Some explanation would help. Is P_m in Figure 1 same as P_{mec} in Figure 2? Furthermore, Figure 2 itself is not clear and needs improvement in drawing. I think the Figures 1 and 2 are copied and pasted from the Simulink of the Matlab, but the Figure 2 could be enlarged for clarity. I have also scanned the page of Figure 2 with marks on it.
- 2) In equation (7), pg. 5, some explanation is needed for the second contributing term to the Torque T , i.e. for the term $0.5(\Delta\omega)$. Why is this 0.5?
- 3) In the second paragraph of pg. 6 from the top, the sentence “The diagram consists of two Proportional Integral Derivative (PID) controllers”. Are these two controllers for the power and speed control?
- 4) In Figure 5, the true and estimated Bode plots are not clear, i.e. a legend is needed to distinguish them.

Modelling micro-turbines using Hammerstein models

Francisco Jurado

University of Jaén, Dept. of Electrical Engineering

23700 Alfonso X, EPS Linares (Jaén), Spain

e-mail: fjurado@ujaen.es Telephone: +34-953-648518 Fax: +34-953-648508

SUMMARY

The Hammerstein model configuration, which includes a nonlinear static block followed by a linear dynamic block, is applied to model the static and dynamic characteristics of the micro-turbine. The parameters in the model can be extracted from the measurements of physical engines or from the simulations of physics-based models. In this paper, a nonlinear model is used to assist dynamic performance of micro-turbines when connected to the grid as distributed generator. *in the the*

KEY WORDS: Hammerstein systems; gas turbines; nonlinear systems; parameter estimation; system identification.

1. INTRODUCTION *of micro-turbines*

The computational burden required for the simulation is highly dependent on the complexity and accuracy of each generator model. The factory need often to provide the user a reliable low-complexity prototype model of the micro-turbine (MT) generator set, sufficiently accurate for the above application. *with simulations*

Gas turbine engines were originally designed for aircraft propulsion, but are now extensively used in industrial applications. With such widespread and increasing applications the modelling of these engines is an issue of some importance. *the great*

use. Engine models are required both in the development and operational stages of the life of a gas turbine. Thermodynamic models are derived during the development stage, based on

^{the} knowledge of ~~the~~ engine physics, and provide important insights into the engine behaviour. Such models are complex, making them unsuitable for use in the design of engine control systems.

At the initial stages of an engine design, a thermodynamic model is derived from the nonlinear differential equations which govern energy transfer within the engine. The nonlinear model is then numerically linearised about a set of operating points, using small perturbations and evaluating the partial derivatives.

Initial work^s on validating small signal engine models ^{were} ~~was~~ carried out in the 1950's on single shaft and twin shaft engines (Lawrence and Powell, 1957; Fitchie *et al.*). Single sine and step inputs were used to excite an engine and domain models calculated. ¹⁹⁵⁹ ?

The results of testing a number of engines with *maximum length binary sequences* (MLBS's) were presented in (Cottingham and Pease, 1979). The amplitude of the perturbation signals was restricted. ^{Another} work examined the application of a range of time-domain methods to estimating ^{estimate} discrete-domain engine models (Hill, 1994). However, ^S some problems with the application of time-domain techniques were reported in a recent paper (Hill, 1997).

The Hammerstein model is a special kind of nonlinear systems which has applications in many engineering problems and therefore, ^{the} identification of Hammerstein models has been an active research topic for a long time. Existing methods in the literature can be roughly divided into six categories: the iterative method (Narendra and Gallman, 1966; Rangan *et al.*, 1995; Voros, 1997), the over-parameterization method (Boutayeb, 1996), the stochastic method (Billings and Fakhouri, 1978; Greblicki, 2000; Krzyzak, 1996; Pawlak, 1991), the nonlinear least squares method (Bauer and Ninness, 2000), the separable least squares method (Bai, 2002 a; Westwick and Kearney, 2001), and the blind method (Bai, 2002 b).

The blind method (Bai, 2002 b) is to use the technique of blind system identification to identify the linear part without requiring the structure of the unknown nonlinearity. A subspace method was proposed in (Favoreel and De Moor, 1999), and Vandersteen *et al.*, 1997 ^P uses periodic signals consisting of a large sinusoidal wave with some small sinusoidal waves. were used in

Frequency domain identification methods for a linear system are well understood and developed (Ljung, 1999; Pintelon and Schoukens, 2001). This idea will be used to for Hammerstein models in this work.

In (Gardiner, 1973), the nonlinearity is assumed to be a polynomial with a known order. For example, in a practical situation, the unknown nonlinearity may be approximated by a polynomial.

This paper deals with the nonlinear identification of the fuel to output power dynamics of a MT. (Sect. 2) presents a review of the MT. (Sect. 3) introduces the Hammerstein model.

Identification of the linear part and identification of the nonlinear part are discussed in Sect. 4. Identification of the MT model is described in Section 5. Sect. 6 depicts some simulation results and some remarks are provided in Section 7.

2. MICRO-TURBINE

A thorough introduction to gas turbine theory is provided in (Cohen *et al.*, 1998). There also exist a large number of publications on the modelling of gas turbines. The model complexity varies according to the intended application. Detailed first principle modelling based upon fundamental mass, momentum and energy balances is reported by (Fawke *et al.*, 1972) and (Shobeiri, 1987). These models describe the spatially distributed nature of the gas flow dynamics by dividing the gas turbine into a number of sections. Throughout each section, the thermodynamic state is assumed to be constant with respect to location, but varying with respect to time. Mathematically, the full partial differential equations model description is reduced to a set of ordinary differential equations, which facilitate easier application within a computer simulation program. For a detailed model, a section might consist of a single compressor or turbine stage. Much simpler models result if the gas turbine is decomposed into just three sections corresponding to the main turbine components i.e. compressor, combustor and turbine, as in (Hussain *et al.*, 1992).

Instead of applying the fundamental conservation equations, as described above, another modelling approach is to characterize the gas turbine performance by utilizing the real steady state engine performance data, as in (Hung, 1991). It is assumed that transient thermodynamic

and flow processes are characterized by a continuous progression along the steady state performance curves, ^{which} this is known as the *quasi-static* assumption. The dynamics of the gas turbine, e.g. combustion delay, motor inertia, fuel pump lag etc. are then represented as lumped quantities separate from the steady-state performance curves. Very simple models result if it is further assumed that the gas turbine is operated at all times close to ^{the} rated speed (Rowen, 1983).

Air at ^{the} atmospheric pressure enters the gas turbine at the compressor inlet. After compression of the air to achieve the most favourable conditions for combustion, ^{the} fuel gas is mixed with the air in the combustion chamber. ^{Then the} combustion takes place and the hot exhaust gases are expanded through the turbine to produce ^{the} mechanical power. In terms of energy conversion, the chemical energy present in the combustion reactants is transferred to the gas stream during combustion. This energy - measured in terms of gas enthalpy- is then converted into ^{the} mechanical work by expanding the gas through the turbine. Thus the excess mechanical power available for application elsewhere, after accounting for the power required to drive the compressor, is derived ultimately from the combustion process.

Compressor power consumption equation **is given by**

$$P_c = \frac{w_a \Delta h_{IC}}{\eta_c \eta_{trans}} \quad (1)$$

Combustion energy equation **is expressed as**

$$w_g c_{pg} (T_{Tin} - 298) + w_f \Delta h_{25} + w_a c_{pa} (298 - T_{cout}) + w_{is} c_{ps} (298 - T_{is}) = 0 \quad (2)$$

Power delivery equation **is written as**

$$P_T = \eta_T w_g \Delta h_{IT} \quad (3)$$

$$P_{mec} = P_T - P_c \quad (4)$$

Figure 1 shows the block diagram of the gas turbine.

$$P_{mec} = T\omega \quad (8)$$

Input variables to the turbine are w_f , $\Delta\omega$ and ω . Output variable from the turbine is P_{mec} . For the purpose of this paper only modulating control of mechanical side of the gas turbine is of interest. The simplified model of the gas turbine controller in this paper consists of two inputs and one output. Inputs to the controller are P_{mec} and ω . The output from the controllers is F_d .

The block diagram of the gas turbine control system is presented in Figure 2 and described by the data in Table 0. The diagram consists of two Proportional Integral Derivative (PID) controllers. *LVG* stands for Least Value Gate that transmitting the minimum of two incoming signals. *transmits*

Figure 2. Gas turbine control system.

Table 0. Micro-turbine Constants.

3. HAMMERSTEIN MODEL

Consider the Hammerstein model shown in Figure 3, where $u(t)$, $v(t)$, $y(t)$ and $y_f(t)$, are the system input, noise, output and filtered output, respectively. $x(t)$ denotes the unavailable internal signal. These are continuous time signals. $u(iT_s)$ and $y_f(iT_s)$ denote the sampled input and sampled filtered output signals respectively with the sampling interval T_s . The filter is a lowpass filter at designer's disposal. *the*

Figure 3. Hammerstein model.

The goal of the frequency domain identification is to apply inputs of the form,

$$u(t) = A \cos(\omega_k t), \quad \omega_k \neq 0, \quad t \in [0, T] \quad (9)$$

and then, to determine a pair of the estimates $\hat{f}(\cdot)$ and $\hat{G}(s)$ based on finite sampled inputs and filtered outputs $u(iT_s)$ and $y_f(iT_s)$ so that the

$$\hat{f}(\cdot) \rightarrow f(\cdot), \quad \hat{G}(s) \rightarrow G(s) \quad (10)$$

in some sense. Note that the continuous time model $\hat{G}(s)$, not its discretised model, is our interest. In fact, the forms of $\hat{f}(\cdot)$ and $\hat{G}(s)$ depend on whether they are parametric or not. Just like the frequency identification approaches for linear systems, the proposed method may also have to be repeated for a number of frequencies.

3.1. Continuous-Time Frequency Response function

The nonlinearity $x = f(u)$ is continuous and piecewise smooth. If the input $u(t) = A \cos(\omega_k t)$ which is an even and periodic function with the period $T = (2\pi)/\omega_k$, then, $x(t)$ is also an even and periodic function that is continuous and piecewise smooth.

and, consequently, x permits a Fourier series representation is possible:
the following

$$x(t) = \sum_{i=0}^{\infty} r_i \cos(i\omega_k t) \quad (11)$$

where the Fourier coefficients are given by

$$r_0 = \frac{\omega_k}{2\pi} \int_0^{2\pi/\omega_k} f(A \cos(\omega_k t)) dt \quad (12)$$

$$r_i = \frac{\omega_k}{\pi} \int_0^{2\pi/\omega_k} f(A \cos(\omega_k t)) \cos(i\omega_k t) dt, \quad i=1,2,\dots \quad (13)$$

Note: Define these in Nomenclature.

3.2. Point Estimation of $G(j\omega)$ Based on Y_T and U_T

The theoretical framework is developed in continuous time domain based on the continuous time model $G(s)$ and continuous time signals $u(t)$, $x(t)$ and $y(t)$. Given the input $u(t) = A \cos(\omega_k t)$, define the point estimate $\bar{G}(j\omega_k)$ of $G(j\omega)$ at $\omega = \omega_k$ as

$$\bar{G}(j\omega_k) = A \frac{\frac{1}{T} Y_T(\omega_k)}{\frac{1}{T} U_T(\omega_k)} \quad (14)$$

where $Y_T(\omega_k)$ and $U_T(\omega_k)$ are the finite time Fourier transforms.

3.3. DFT Implementation

The Discrete Fourier Transforms (DFTs) of $u(iT_s)$ and $y_f(iT_s)$ are defined by $Y_{f,DFT}(\omega_k)$ and $U_{f,DFT}(\omega_k)$. The point estimate $\bar{G}_d(j\omega_d)$ using only the sampled $u(iT_s)$ and $y_f(iT_s)$ is determined by

$$\bar{G}_d(j\omega_k) = A \frac{Y_{f,DFT}(\omega_k)}{U_{f,DFT}(\omega_k)} \quad (15)$$

4. IDENTIFICATION

4.1 Linear part

Given the point estimates $\bar{G}_d(j\omega_d)$'s, to find a $G(j\omega)$ is a curve fitting problem. Whether a particular method is effective for identification of $G(j\omega)$ depends on the

assumptions of $G(j\omega)$. If $G(j\omega)$ is nonparametric, it is expected that the method is complicated and tedious. On the other hand, the identification is much easier if the unknown $G(j\omega)$ is known to be an n th-order rational transfer function.

When the unknown $G(j\omega)$ is characterized by an n th-order stable rational transfer function

$$G(s) = \frac{b_1 s^{n-1} + b_2 s^{n-2} + \dots + b_n}{s^n + a_1 s^{n-1} + a_2 s^{n-2} + \dots + a_n} \quad (16)$$

The unknown coefficient vector θ and its estimate $\hat{\theta}$ are denoted by

$$\begin{aligned} \theta &= (b_1, \dots, b_n, a_1, \dots, a_n)', \\ \hat{\theta} &= (\hat{b}_1, \dots, \hat{b}_n, \hat{a}_1, \dots, \hat{a}_n)' \end{aligned} \quad (17)$$

The simplest way to find $\hat{\theta}$ is to solve the least squares minimization (Levi, 1959). Let

$$e(\hat{\theta}, \omega_k) = \overbrace{G(j\omega_k)}^{G(j\omega_k)} - \bar{G}_d(j\omega_k) \left((j\omega_k)^{n-1} \hat{b}_1 + \dots + \hat{b}_n \right) - \bar{G}_d(j\omega_k) \left((j\omega_k)^{n-1} \hat{a}_1 + \dots + \hat{a}_n \right) \quad (18)$$

and so, the estimate $\hat{\theta}$ is obtained by

$$\hat{\theta} = \arg \min \sum_{k=1}^N \|e(\hat{\theta}, \omega_k)\|^2 \quad (19)$$

for some $N > n$. Clearly, if $\bar{G}_d(j\omega_k) = G(j\omega_k)$, $e(\theta, \omega_k) = 0$ and $\hat{\theta} = \theta$.

then, the estimate $\hat{G}(s)$ is defined as

$$\hat{G}(s) = \frac{\hat{b}_1 s^{n-1} + \dots + \hat{b}_n}{s^n + \hat{a}_1 s^{n-1} + \dots + \hat{a}_n} \quad (20)$$

→ The least squares solutions $\hat{G}(j\omega)$ of (19) and (20) are consistent ^{with the} (in) theory because $\bar{G}_d(\omega_i) \rightarrow G(j\omega)$ as $T \rightarrow \infty$.

4.2 Nonlinear part

When the linear part $\hat{G}(s)$ is identified, the nonlinear part $\hat{f}(u)$ can be estimated. There are two cases: 1) there is no *a priori* knowledge on the structure of the unknown $f(u)$ and 2) $f(u)$ is represented by a polynomial with a known order. In both cases, it is required to estimate the Fourier coefficients r_i 's. This paper studies a simple case when the unknown nonlinearity is parameterized by a polynomial

$$x = \sum_{i=0}^l \beta_i u^i \quad (21)$$

The exact order of the polynomial is not necessarily known. However, an upper bound l is assumed to be available.

Denote

$$l_1 = \left[\frac{l}{2} \right] \quad l_2 = \left[\frac{l}{2} \right] - \text{rem}(l+1, 2) \quad (22)$$

where $[l/2]$ rounds $l/2$ to the nearest integer toward zero and $\text{rem}(l+1, 2)$ is the remainder after division $(l+1)/2$. When $u(t) = A \cos(\omega_c t)$ it follows that

with

$$x(t) = \sum_{i=0}^l \beta_i u^i(t) = \sum_{i=0}^{l_1} r_i \cos(i\omega_c t) \quad (23)$$

hence, the estimates $\hat{\beta}_i$'s and $\hat{f} = \sum_{i=0}^l \hat{\beta}_i u^i$ can be easily obtained based on the estimates of \hat{r}_i 's, and

$$\hat{f}(u) = \sum_{i=0}^l \hat{\beta}_i u^i \quad (24)$$

Clearly, if $\hat{r}_i \rightarrow r_i$ in probability as $T \rightarrow \infty$, then $\hat{\beta}_i \rightarrow \beta_i$ and $\sup_{u \in [-A, A]} |\hat{f}(u) - f(u)| \rightarrow 0$ in probability as $T \rightarrow \infty$.

5. IDENTIFICATION OF THE MICRO-TURBINE MODEL

A second-order term is sufficient to model the static nonlinear behaviour of the engine and the linear part is a second order transfer function. The noise $v(t)$ is a random signal uniformly distributed and the input is

$$u(t) = A \cos(\omega_i t), \quad A = 1, \quad i = 1, 2, 3$$

with $\omega_1 = 0.6$, $\omega_2 = 1.2$, $\omega_3 = 6$ and $T_s = 100((2\pi)/\omega_i)$. For ^{the} input frequency ω_i , the sampling interval is set to be $\pi/(50\omega_i)$. No lowpass filter is used in simulation, ^si.e., $y(t) = y_f(t)$. Because the linear part is parametric, we use the estimate of (12). Thus, the estimates of $\hat{f}(\cdot)$ and $\hat{G}(s)$ are given by

$$f(u) = 0.0016u^2 + 0.6067u + 2.301$$

$$G(s) = \frac{0.0449s + 0.0068}{s^2 + 0.4753s + 0.0531}$$

which are very close to the true but unknown $f(u)$ and $G(s)$. The true (solid line) and the estimated (circle) nonlinearities are shown in Figure 4, and the Bode plots of the true and the estimated transfer functions are shown in Figure 5. They are basically indistinguishable.

Figure 4. True (solid) and the estimated (circle) nonlinearities.

Figure 5. Bode plots.

6. SIMULATION RESULTS

The IEEE test feeders (Kersting, 2001) are used as the test systems to investigate the dynamic characteristics of the distribution system with MTs. Figures 6 and 7 show the test systems with the MTs.

In this paper, all loads are balanced, and characterized by constant power. The MT is natural gas operated, with the ratings of 100 kW electric and 167 kW thermal outputs (Aglén, 2001; Chee-Mun, 1998). This unit is eminently well suited as a power source for facilities ranging from hospitals and hotels to shopping malls and factories. The heart of the unit is a small gas turbine which is integrated with a high-speed generator.

Here, every MT has the same parameters. All the MTs are regarded as coherent machines, which have the same dynamic response and share the generation equally. The entire electrical system was modelled dynamically with MATLAB™.

Figure 6. One line diagram of IEEE 13 node test feeder with MTs.

Figure 7. One line diagram of IEEE 34 node test feeder with MTs.

Figure 8 shows the response characteristics to a three-phase bolted fault applied to node 680 in the IEEE 13 node test feeder at $t = 0.5$ s. Distributed generator DG3 is tripped after

the application of the fault. The fault is cleared at $t = 0.8$ s. This figure depicts the mechanical power for DG1, dropping to near zero. Stability returns after 4 s. This response, at the time the disturbance was applied, compares favourably to the expected characteristic MT performance.

Figure 8. MT mechanical power response to bolted three-phase bus fault. Loss of one MT generator.

The next study case simulates MT operating in the IEEE 34 node test feeder. The test involved intentionally tripping one of generator and observing the response of the remaining generators. At $t = 0.5$ s, DG6 is tripped off-line. Figure 9 shows unit DG1 going to full power. This response matched very closely to that which was observed in the full model. The lag in the response to the mechanical power output following the load shedding is due to the energy required to restore the system frequency to 60 Hz, in addition to supplying the required load demand. Stability returns after 5 s.

Figure 9. Mechanical power loss of one MT generator.

Figure 10 shows the node voltage dynamic response characteristics. The two levels of load shedding are evident from the steep slope increases at $t = 0.8$ s and $t = 1.9$ s, as shown. The overshoot in bus voltage magnitude is due to the generator exciter response characteristics.

Figure 10. Voltage dynamic response characteristics. Loss of one MT generator (no load shedding).

This test case is similar to the previous test case, except that no load shedding is performed. Frequency decay is evident. Figure 11 shows the mechanical power, unit remains at maximum power, which is able to satisfy the electrical system load demand. This condition will eventually lead to generator tripping off-line.

Figure 11. Mechanical power loss of one generator (no load shedding).

7. CONCLUSIONS

To determine the potential impacts of ^{the} MTs on future distribution system, dynamic models of ^{the} MTs should be created, ~~reduced in order~~, and scattered throughout test feeders. ^s reduced-order

A frequency domain identification approach for Hammerstein models is proposed in this paper. By exploring the fundamental frequency, the linear ~~part~~ and the nonlinear ~~part~~ ^s can be identified.

The entire distribution system has been modelled dynamically and tested with various operating configurations and electrical disturbances. Evaluation of MT performance was possible with this dynamic modelling. ^{the}

^{shown to be}

NOMENCLATURE

a, b, c	valve parameters
c_{pa}	specific heat of air at constant pressure (J/(kg K))
c_{pg}	specific heat of combustion gases (J/(kg K))
c_{ps}	specific heat of steam (J/(kg K))
e_1	valve position
F_d	fuel demand signal
K_I	PID parameter
K_P	PID parameter
k_f	fuel system gain constant
k_{LHV}	factor which depends on LHV
LHV	lower heating value (MJ/kg)
P_c	compressor power consumption (W)
p_{cin}	air pressure at compressor inlet (Pa)

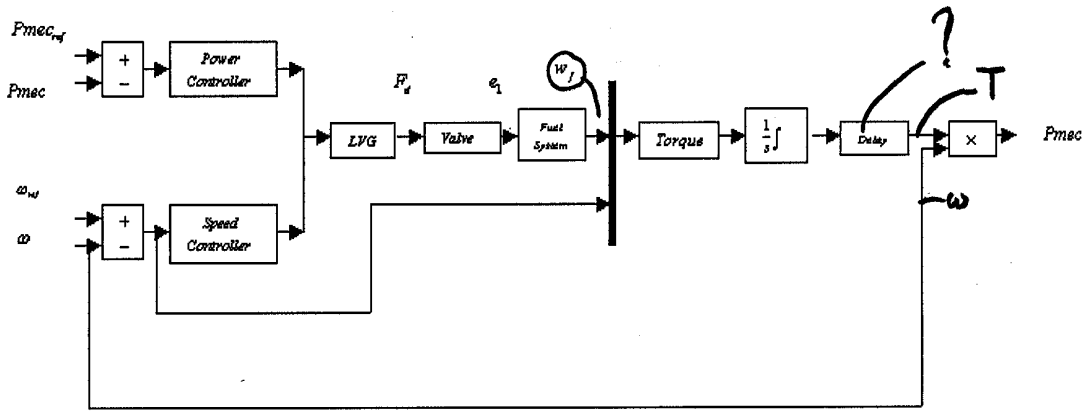


Figure 2. Gas turbine control system.

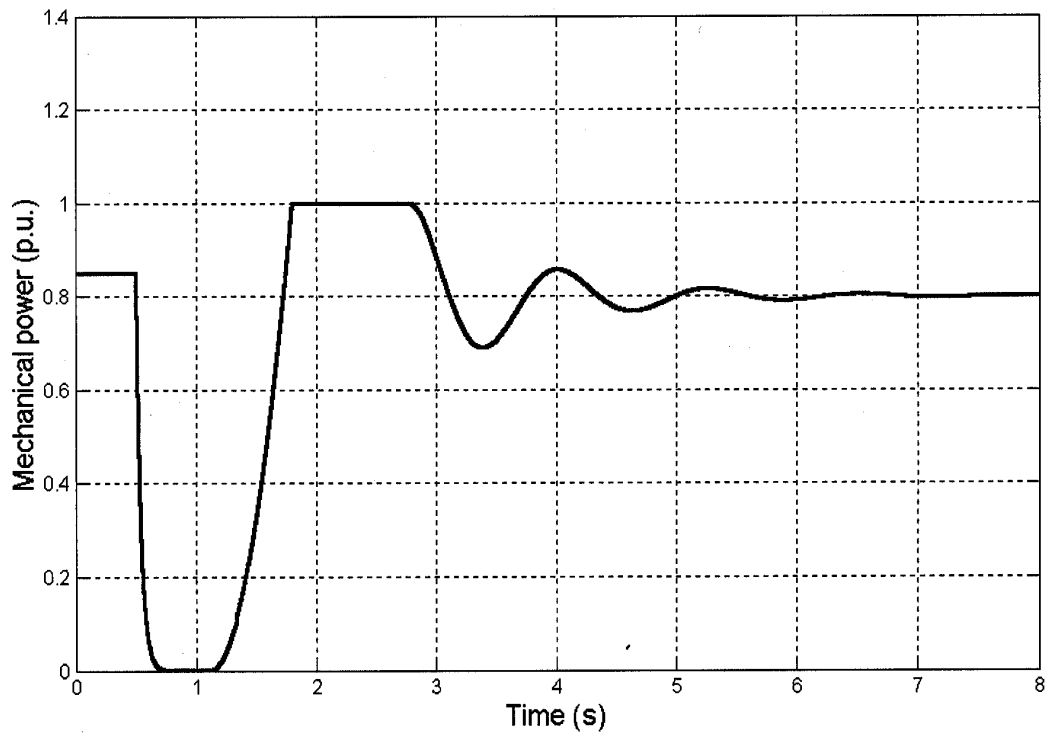


Figure 8. MT mechanical power response to bolted three-phase bus fault. **Loss**
of one MT generator.

Table 1 Micro-turbine constants.

a	b	c	k_f	τ_f
1	0.05	1	1	0.4